

SUPPORTING INFORMATION

OF

Transfer of Epitaxial SrTiO₃ Nanothick Layers Using Water-Soluble Sacrificial Perovskite Oxides

*Yoan Bourlier^{*1,2}, Bruno Bérini¹, Mathieu Frégnaux², Arnaud Fouchet³, Damien Aureau²,
and Yves Dumont¹*

¹ Groupe d'Etude de la Matière Condensée (GEMaC), Université de Versailles Saint-Quentin en Yvelines, Université Paris-Saclay CNRS, 45 avenue des Etats-Unis, 78035, Versailles, France

² Institut Lavoisier de Versailles (ILV), Université de Versailles Saint-Quentin en Yvelines, Université Paris-Saclay CNRS, 45 avenue des Etats-Unis, 78035, Versailles, France

³ NORMANDIE UNIV, ENSICAEN, UNICAEN, CNRS, CRISMAT, 14000 CAEN, France

Corresponding Author : Yoan Bourlier, yoan.bourlier@uvsq.fr

KEYWORDS: SrVO₃, SrTiO₃ pseudo-substrate, sacrificial layer, silicon, water soluble

Afm_SVO dissolution_movie.mpeg

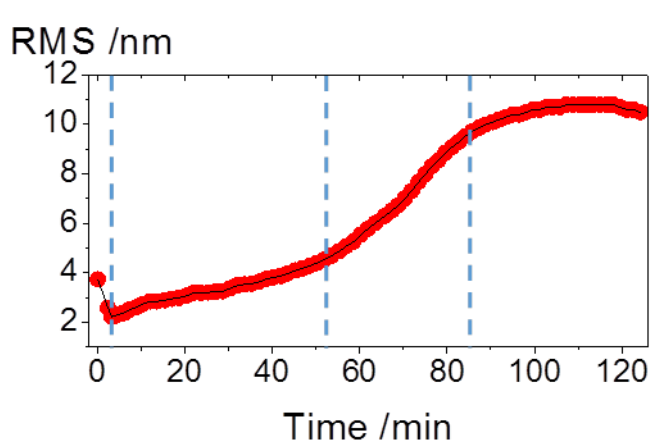


Figure S1: Video of *in situ* AFM (in liquid-mode) of the SrVO₃ (SVO) thin film dissolution in water with surface nanostructured (WMV) and associated roughness (root mean square or RMS) evolution in time. The *in situ* AFM video starts with a first AFM image taken in air environment and a second AFM scan at a time of 2 min 20 sec (time used for settings). The acquisition time was set to 100 sec per analysis (see the experimental part for more information details). At the beginning, from 0 min to 3 min in water, RMS decreases from 3.7 nm to 2.2 nm which is due to the fast dissolution of the Sr-rich nanostructures leaving their imprints down to surface. Then, the RMS increases slightly, with a constant slope until 52 min (RMS around 4.5 nm), and with a higher slope from 52 min to 85 min until a RMS of 9.7 nm. The first increase of roughness is explained by the dissolution of the film, taking place around the nanoimprints of the former nanostructures. Concerning the second RMS increase, such higher slope is accompanied by a higher dissolution speed of the film which starts to decompose in “aggregates” or “particles”. Finally, a steady state of the RMS around 10.8 nm after 85 min with a low decrease after 120 min is observed. This last step is associated to the almost complete dissolution of the SVO thin film with the grading appearance of the SrTiO₃ (STO) substrate. A mechanical removal effect of the tip is also supposed to etch particles from the surface.

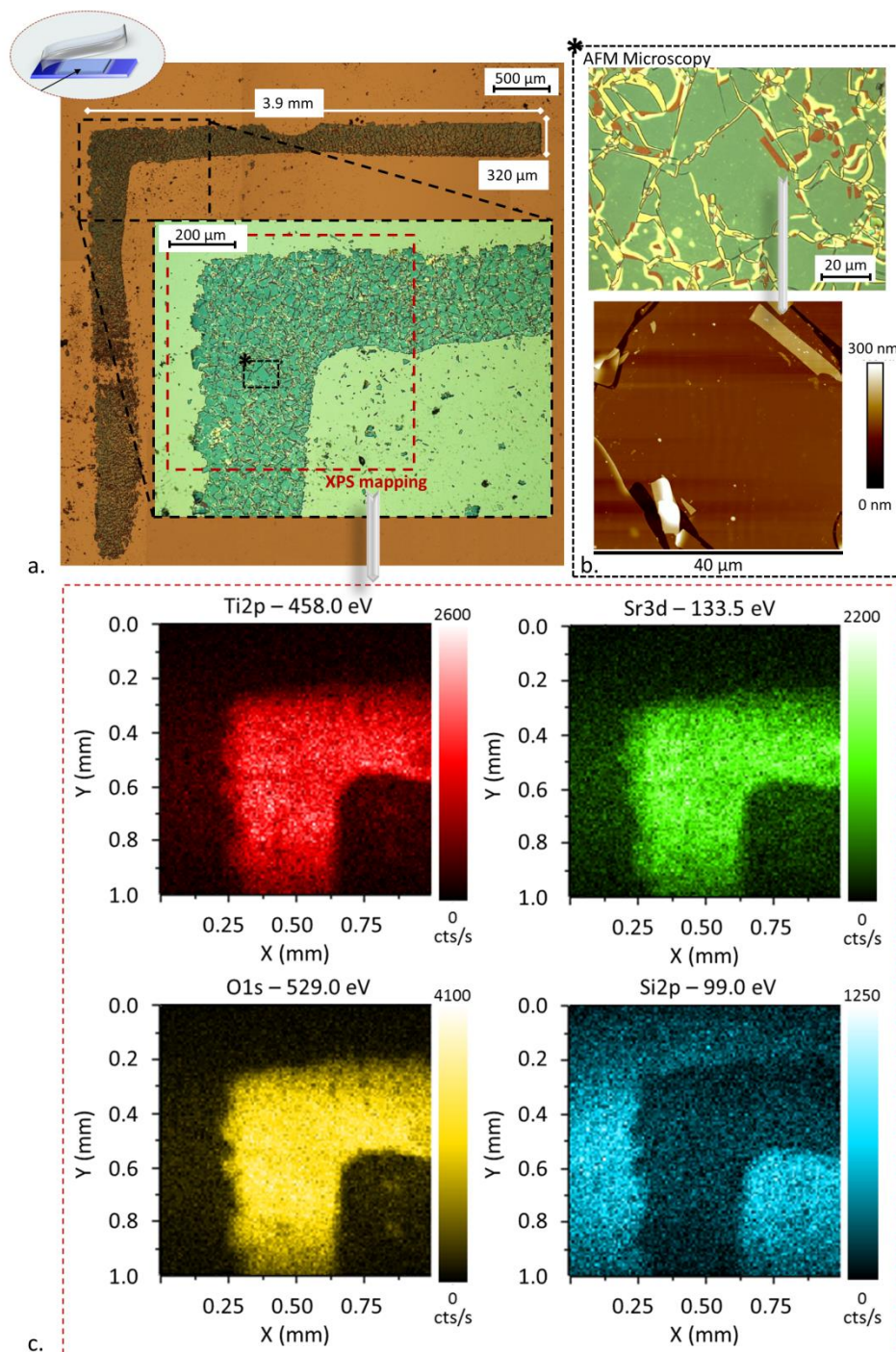


Figure S2: STO-transferred thin film onto Si substrate using PDMS support, (a) Optical micrographs reconstruction of the transferred layer with zoom of the particular zone of interest; (b) focused zone micrograph with corresponding AFM analysis of the area, and (c) XPS mapping of the related zone of interest showing Ti2p, Sr3d, O1s, and Si2p spectral signature.

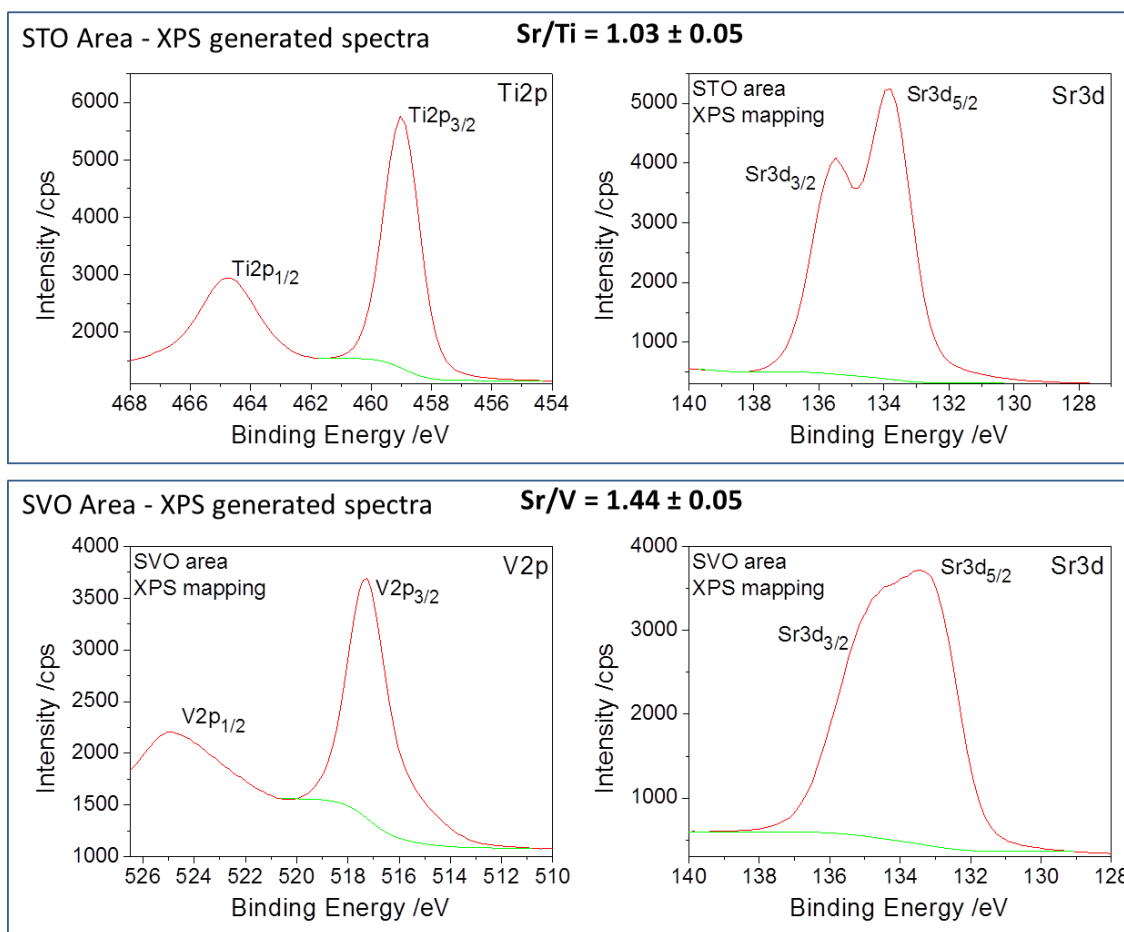


Figure S3: High energy resolution spectra of (Ti2p, Sr3d) and (V2p, Sr3d) on STO focused area and SVO focused area, generated from XPS mapping (related to figure 2) on the sample before processing the transfer. The standard error deviation of the Sr/Ti and Sr/V ratios is around ± 0.05 .

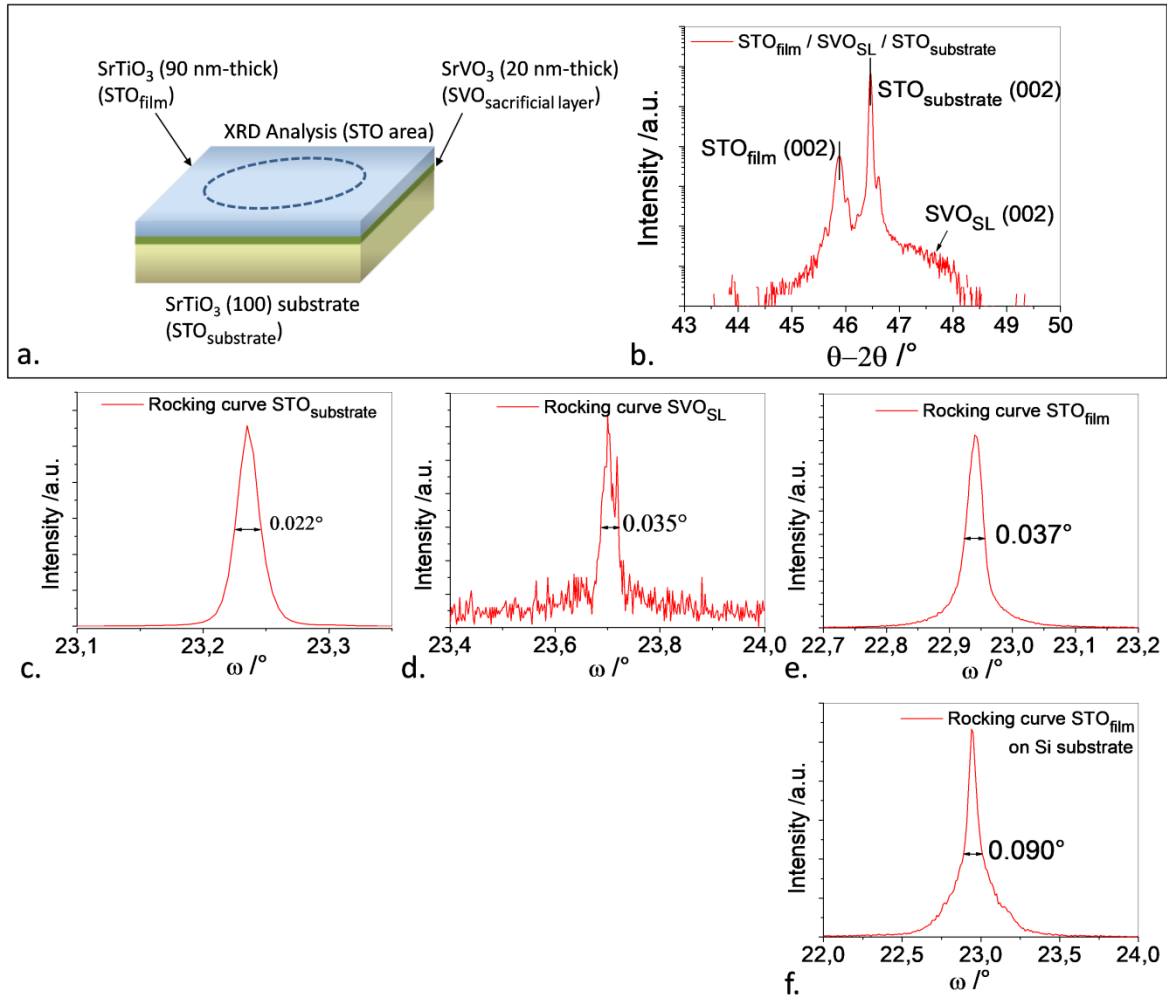


Figure S4: XRD analyses with rocking curves of (002) Bragg peaks (a) Layout of the “STO_{film}/SVO_{SL}/STO_{substrate}” stack (STO focused area) with (b) XRD θ - 2θ analysis associated and centered on the (002) Bragg peaks. **From (c) to (e):** Rocking curves related to XRD analysis of the stack, associated to Bragg peaks of (c) STO_{substrate}(002), (d) SVO_{SL}(002), and (e) STO_{film}(002). **And (f):** Rocking curve related to XRD analysis of the final STO-transferred thin film onto Si substrate (presented in **Figure 5d**) associated to Bragg peak STO_{film}(002).

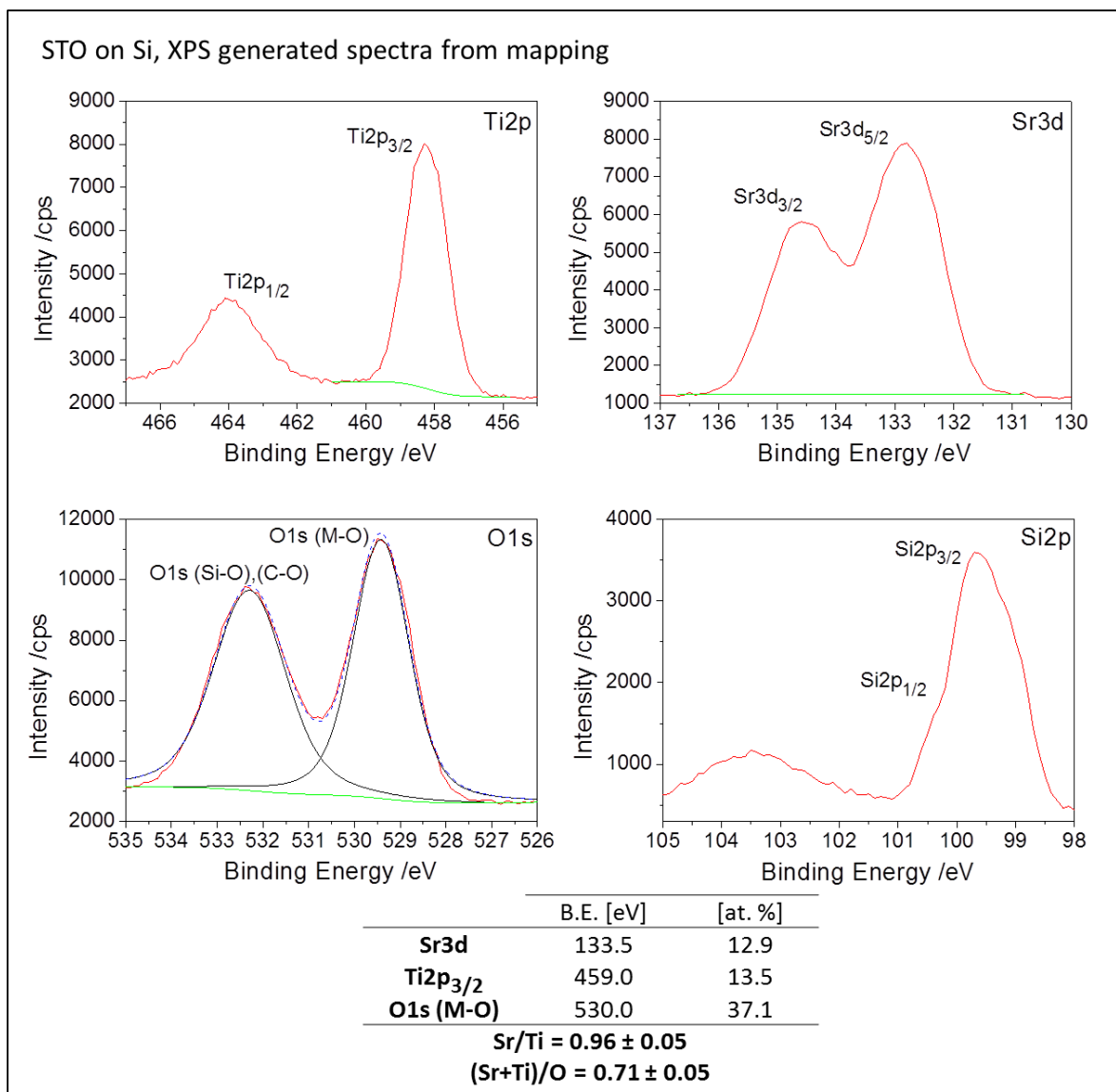


Figure S5: High energy resolution spectra of Ti2p, Sr3d, O1s, and Si2p on STO-transferred thin film onto silicon substrate, generated from XPS mapping (related to figure 4) on the sample after processing the transfer. The standard error deviation of the Sr/Ti and (Sr+Ti)/O ratios is around ± 0.05 .

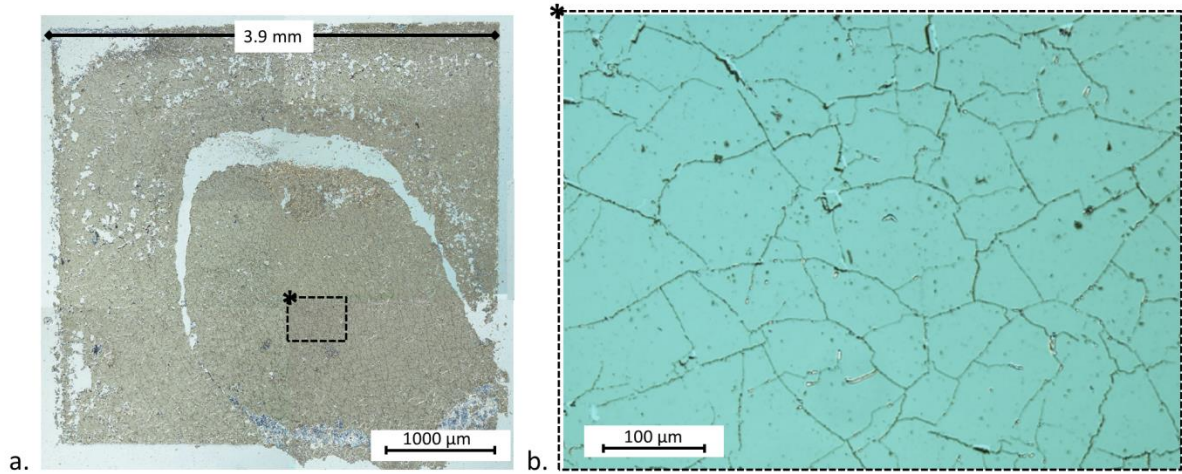


Figure S6: 20 nm-thick STO-transferred thin film onto Si substrate, (a) optical micrograph reconstruction of the STO-transferred layer, and (b) micrograph of a particular zone of interest.

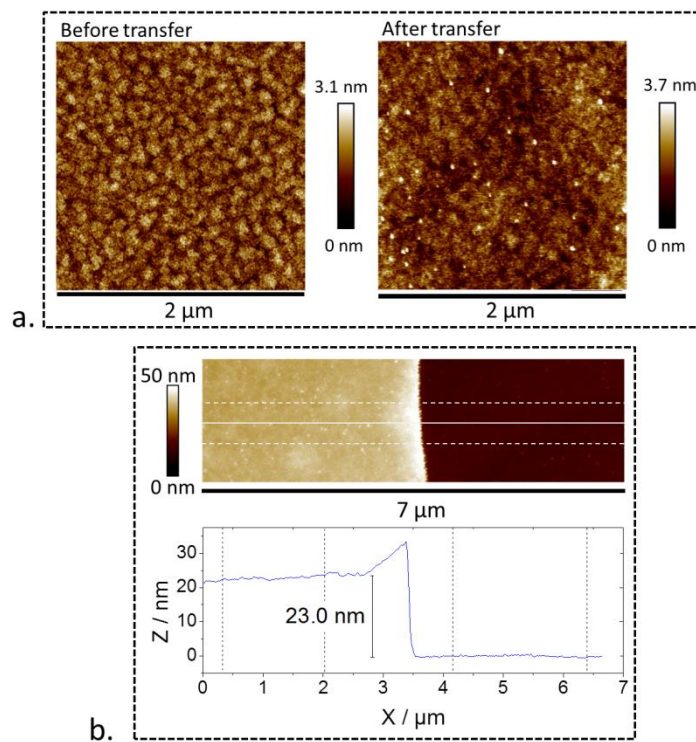


Figure S7: 20 nm-thick STO-transferred thin film onto Si substrate, (a) AFM roughness analysis before transfer (RMS=0.46 nm) and after transfer (RMS=0.53 nm), and (b) AFM thickness measurement giving an average thickness of 23.0 nm. The $2 \times 2 \mu\text{m}^2$ AFM image is representative to a well-preserved smooth and homogeneous surface with a conserved thickness.

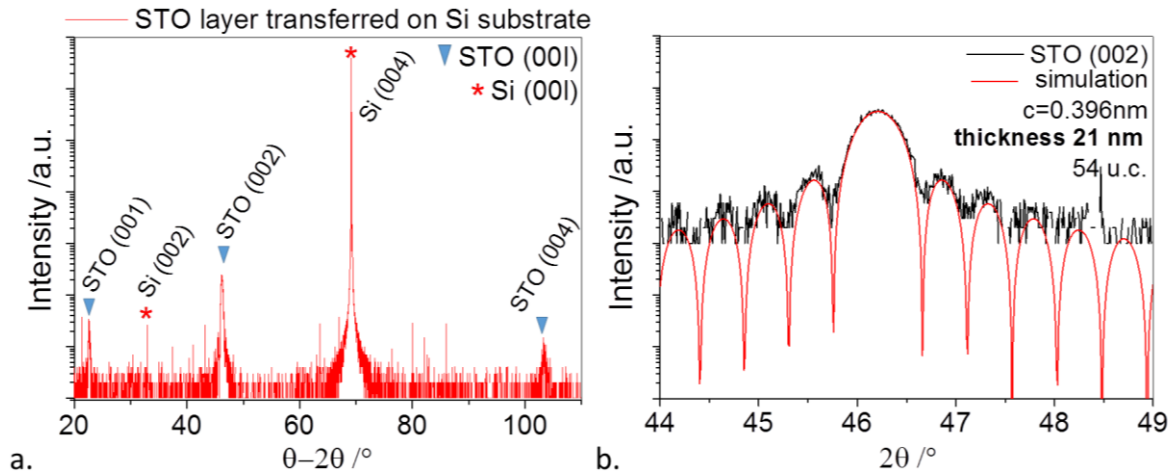


Figure S8: 20 nm-thick STO-transferred thin film onto Si substrate, (a) X-ray $\text{Cu K}\alpha_1$ diffractogram of the STO transferred layer, and **(d)** X-ray Laue oscillations near the STO (002) diffraction peak. Bragg peaks at 2θ angles of 32.97° , and 69.14° are associated to Si substrate (002) and (004) planes, respectively. STO Bragg peaks corresponding to (001), (002), and (004) indexes, are visible at 2θ angles of 22.65° , 46.24° , and 103.47° , respectively. It proves that the STO-transferred layer is well crystallized with its original preferential orientation preserved, following the (001) crystalline planes. The Laue oscillations from STO (002) peak gives a corresponding lattice parameter of $c = 0.396 \text{ nm}$ and a number of 54 unit-cells. The resulting thickness estimation of 20 nm is in perfect agreement with the ones calculated from AFM height scan and estimated from PLD process conditions. Furthermore, these well-resolved Laue oscillations up to high order confirm the atomic flatness of the STO in the rear face and the good quality of an intimate STO/Si interface.